AJNR

Neonatal Citrullinemia: Comparison of Conventional MR, Diffusion-Weighted, and Diffusion Tensor Findings

Charles B. L. M. Majoie, Jeroen M. Mourmans, Erik M. Akkerman, Marinus Duran and Bwee Tien Poll-The

AJNR Am J Neuroradiol 2004, 25 (1) 32-35
http://www.ajnr.org/content/25/1/32

AJNR Am J Neuroradiol 25:32–35, January 2004

Case Report

Neonatal Citrullinemia: Comparison of Conventional MR, Diffusion-Weighted, and Diffusion Tensor Findings

Charles B. L. M. Majoie, Jeroen M. Mourmans, Erik M. Akkerman, Marinus Duran, and Bwee Tien Poll-The

Summary: Conventional MR, diffusion-weighted, and diffusion tensor imaging were performed in an 8-day-old girl with citrullinemia. She had severe hyperammonemia for several days. On conventional T2-weighted MR images, symmetric, confluent high signal intensity was found in the bilateral thalami, basal ganglia, cortex, and subcortical white matter. Diffusion-weighted imaging demonstrated decreased apparent diffusion coefficient in these areas, reflecting cytotoxic edema. Follow-up MR imaging at the age of 4 months revealed subcortical cysts, ulegyric changes, and atrophy, which were most prominent in the occipital lobes. Diffusion tensor imaging revealed decreased anisotropy throughout the brain, consistent with diffuse injury to the oligodendro-axonal unit. Diffusion-weighted and diffusion tensor imaging are valuable techniques for the detection of irreversible brain damage and for the characterization of hyperintense lesions on T2-weighted MR images in patients with the neonatal form of citrullinemia.

Citrullinemia is one of the urea cycle disorders, caused by argininosuccinic acid synthetase deficiency (ASS), with an estimated incidence of 1/57,000 live births (1). The diagnosis of citrullinemia is based on biochemical analysis of blood, plasma, and urine, revealing increased levels of ammonia, citrulline, glutamine, and orotic acid. ASS enzyme activity can be assayed in liver samples and cultured fibroblasts (2). In neonatal-onset disease, neonates exhibit lethargy and vomiting 24–72 hours after birth, rapidly progressing to respiratory insufficiency and coma.

Neurodevelopmental outcome of neonatal urea cycle defects is disappointing and is related to the duration of neonatal hyperammonemic coma. There is, however, no consensus regarding other early prognostic indicators.

Reports on imaging findings in citrullinemia are sparse. A recent article describes CT findings in two infants in the chronic stage of this disease (2). Other studies describe MR findings in the adult form (3–6). We report the MR abnormalities of the neonatal form of citrullinemia on conventional T2-weighted images of serial MR images and compare these with findings on diffusion-weighted and diffusion tensor images.

Received January 3, 2003; accepted after revision April 28.

From the Departments of Radiology (C.B.L.M.M., E.M.A.) and Pediatric Neurology (J.M.M., B.T.P.-T.) and Laboratory of Genetic Metabolic Diseases (M.D.), Academic Medical Center, Amsterdam, the Netherlands

Address correspondence to Dr. Charles B. L. M. Majoie, Department of Radiology, Academic Medical Center, P.O. Box 22660, 1100 DD Amsterdam, the Netherlands.

Case Report

The patient was born as the first child of nonconsanguineous parents after an uneventful pregnancy and delivery. On day 2 of life, she started vomiting and became lethargic. On day 5 she was transferred to our hospital because of convulsions and respiratory insufficiency. Metabolic screening revealed hyperammonemia (882 μmol/L; normal, <100 μmol/L). Citrullinemia was diagnosed on the basis of blood values of citrulline (2874 μmol/L; normal, 5–33 μmol/L), arginine (9 μmol/L; normal, 12–166 μmol/L), and glutamine (3067 μmol/L; normal, 198–866 μmol/L) and massive urinary excretion of citrulline and orotic acid. Although treatment was started with a high-calorie diet and supplementation of arginine, sodiumbenzoate, and carnitine, blood ammonia reached a peak level of 2083 μmol/L 1 day later. With peritoneal dialysis for 1 day, blood ammonia, and glutamine levels normalized on day 8, but she was still comatose.

MR imaging of the whole brain was performed on day 8 on a 1.5-T system (Vision; Siemens, Erlangen, Germany) equipped with a standard quadrature head coil. Conventional spin-echo T1-weighted (570/14 [TR/TE]) and fast spin-echo T2-weighted (3500/22–90 [TR/TE_{eff}]) images were obtained with an echo train length of 10, a field of view of 23 × 23 cm, an imaging matrix of 256 × 256, and a 5-mm section thickness with a 1-mm gap. Diffusion-weighted MR images were acquired with a field of view of 26 × 26 cm. Section thickness, gap, orientation, and section positions were the same as in those in the axial T1- and T2-weighted sequences. We used a single-shot, spin-echo, echo-planar sequence, with a TE of 100 ms, an acquisition matrix of 96 × 200, reconstructed to 256 × 256 images. One image with a b value of 0 was acquired, and six images with a b value of 1000 s/mm^2, with the diffusion sensitizing gradient pointing in six noncollinear directions, so as to gather complete diffusion tensor data. The TR between echo planar acquisitions was 4000. From the acquired data, the average apparent diffusion coefficient (ADC) was calculated—ie, one-third the trace of the diffusion tensor and the fractional anisotropy (7).

Axial T2-weighted images showed symmetrical high signal intensity in the temporal, parietal, and occipital cortex and subcortical white matter and in both caudate nuclei, thalami, internal capsules, and the globus pallidus (Fig 1A). Diffusion-weighted images showed high signal intensity (Fig 1B) and low ADC (Fig 1C) values in these regions, consistent with cytotoxic edema. The patient was comatose and was ventilated for 6 days. Thereafter, hyperammonemic episodes did not recur, but she remained hypotonic and neurologically depressed for 2

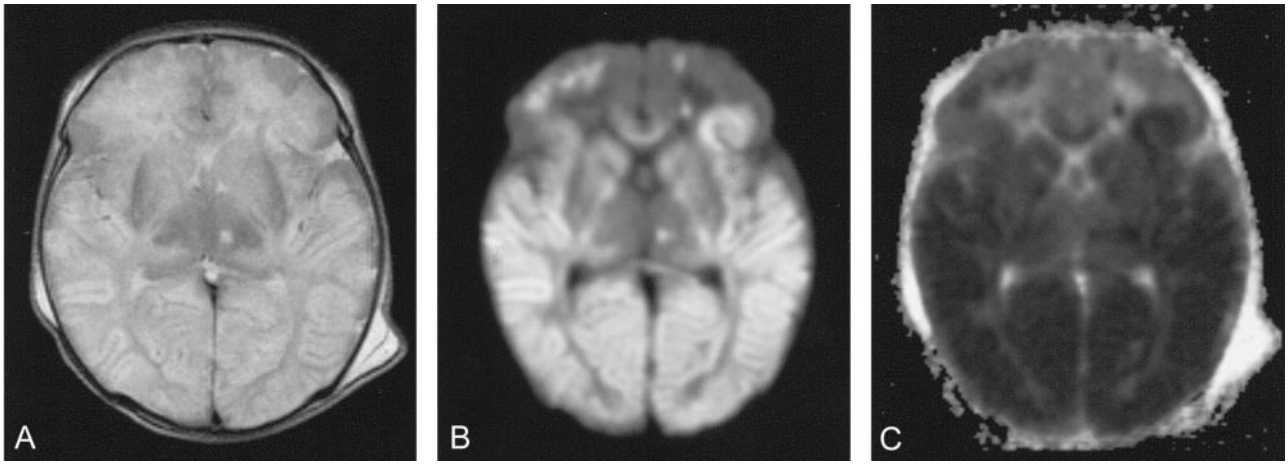

FIG 1. Images from the case of a 8-day-old girl with citrullinemia. MR imaging was performed 2 days after a blood ammonia peak of 2083 μmol/L.

A, Axial fast spin-echo T2-weighted MR image (3500/90/1) shows high signal intensity in the bilateral basal ganglia, thalami cortex, and subcortical white matter.

B, Diffusion-weighted MR image demonstrates restricted diffusion in these areas.

C, ADC map corresponding to area shows decreased ADC in these areas consistent with cytotoxic edema.

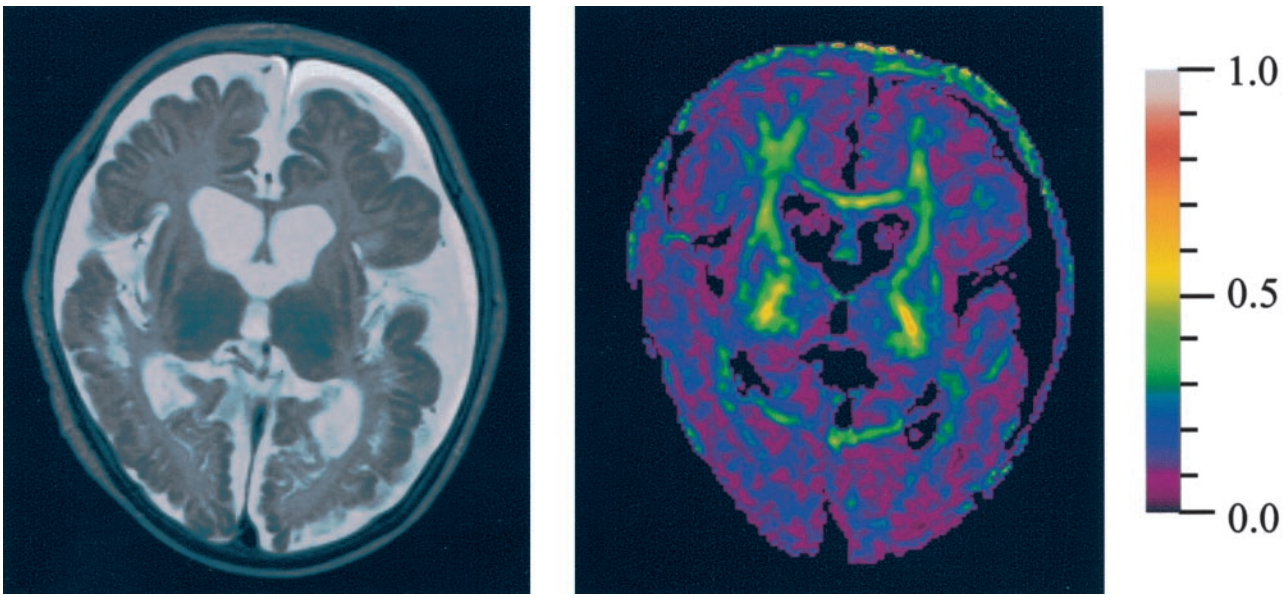

FIG 2. Follow-up MR imaging at age 4 months, when the patient had severe neurodevelopmental delay.

A, Axial fast spin-echo T2-weighted MR image (3500/90/1) shows atrophy, ulegyric changes, and subcortical cysts, especially in the occipital lobes.

B, Color-coded fractional anisotropy map demonstrates fractional anisotropy (FA) decrease throughout the brain. Red refers to FA = 1 and purple to FA = 0.

weeks. Follow-up at 4 months showed microcephaly and severe neurodevelopmental delay with generalized hypotonia, head lag, and hyperreflexia. She failed to make visual contact, and her pattern of movements was stereotyped.

Metabolic tests and MR imaging were repeated at the age of 4 months. In blood, ammonia was 29 μmol/L (normal, <50 μmol/L); citrulline, 3081 μmol/L (normal, 6–34 μmol/L), and glutamine, 702 μmol/L (normal, 333–809 μmol/L). Cerebrospinal values were as follows: citrulline, 446 μmol/L (normal, 1.2–7.8 μmol/L) and glutamine, 445 μmol/L (normal, 390–824 μmol/L). Axial T2-weighted MR images showed extensive tissue loss, ulegyric changes, and subcortical cysts, especially in the occipital lobes (Fig 2A). Diffusion tensor imaging revealed decreased anisotropy throughout the white matter of the whole brain (Fig 2B) as compared with normal brain.

Discussion

Enzyme abnormalities in citrullinemia patients are classified into three types (8). The classic neonatal or infantile form is divided into type I (abnormal kinetics of the enzyme) and type III (undetectable or extremely low levels of the enzyme). For types I and III, 22 mutations have been identified in the ASS gene locus (3). The neonatal form is usually severe and has a high mortality rate. The infantile form presents after the age of 5 months and usually has a mild clinical course. Type II occurs almost exclusively in adults and is caused by a decreased level of ASS with

normal kinetic properties in the liver, but normal ASS activities in other tissues such as the kidney, brain, and fibroblasts. In type II, no mutation has been discovered within the ASS gene locus.

As in other urea cycle disorders, the inability to produce urea leads to hyperammonemia and glutamine accumulation, causing astrocyte swelling and encephalopathy (1, 9–11). In the neonatal form, the acute presentation occurs within days or hours of birth and is characterized by progressive neurologic deterioration (12). This presentation can be confused clinically with severe hypoxic ischemic encephalopathy. On the basis of an animal model of hyperammonemic coma, it is believed that astrocytes are the sites of incorporation of ammonium into glutamine through the action of glutamine synthetase, resulting in an increase of their osmolality and cellular swelling (10, 11). Hypercitrullinemia itself is possibly also neurotoxic by the inhibition of aerobic glucose metabolism, as suggested by Okken et al (13). If this disorder is not recognized early and treated promptly, death may follow cerebral edema, elevated intracranial pressure, and herniation (1, 10–12).

Previous studies have described MR findings in the adult form of citrullinemia (1, 3–6). These findings included hyperintensities on T2-weighted images in the cerebral white matter (1), cingulate gyri, temporal lobes and insular regions (4, 5), pons, and cerebellar peduncles (3) and reversible areas of focal cerebral edema (6).

The current report describes MR imaging findings in a neonate with citrullinemia, both in the subacute stage and at the 4-month follow-up. In the subacute stage, axial T2-weighted images showed symmetrical high signal intensity of the temporal, parietal, and occipital cortex and subcortical white matter in caudate nuclei, thalami, internal capsules, and the globus pallidus. Diffusion-weighted images showed high signal intensity and low ADC values in these regions, consistent with cytotoxic edema. When the patient was 4 months old, we found atrophy, ulegyric changes, and subcortical cysts in the bilateral temporal, occipital, and parietal lobes. In contrast to reported findings in the infantile form of citrullinemia (9, 10), in our patient with the neonatal form, the abnormalities were most prominent in the occipital lobes. Diffusion tensor imaging demonstrated fractional anisotropy decrease throughout the brain, not only in the occipital, temporal, and parietal white matter, but also in the corpus callosum and internal capsules. It is possible that fiber destruction, demyelination, and Wallerian degeneration contributed to the decrease of anisotropy in these areas. In the normal brain, diffusion is anisotropic (7, 14). The cause of anisotropy in the brain is not completely understood. It is likely that different factors contribute to anisotropy, including axonal direction, myelination, axolemmelic flow, extracellular bulk flow, capillary blood flow, and intracellular streaming (15). Anisotropic diffusion has been shown before the onset of myelination in the developing rat brain. This premyelination anisotropy seems to be related to some premyelinative changes, including an increase in fiber diameter, axonal membrane changes, and ensheathment of axons by oligodendrocytes (16).

Neuropathologic studies in hyperammonemic disorders reveal predominantly astrocytic changes consisting of cell swelling in acute hyperammonemia and Alzheimer type II astrocytosis in chronic hyperammonemia (9, 11). Hyperammonemia has profound effects on brain metabolism and perfusion (11). Acute hyperammonemia leads to increased cerebral blood flow and accumulation of lactate in the brain. Chronic mild hyperammonemia may lead to region-selective alterations of the cerebral metabolic rate for glucose (11). Martin et al (9) described the neuropathologic findings in an 11-month-old citrullinemic infant. Macroscopic examination revealed frontoparietal ulegyria with relative sparing of the occipital lobe, cortico-subcortical necroses with microcavitation, and ventricular dilatation. Microscopic examination showed multiple cortical necroses and subcortical and axial white matter involvement with demyelination, dense fibrillary gliosis, and lipid-laden macrophages. Confluence of subcortical lesions produced microcystic or polycystic cavities. These findings were found predominantly in the frontotemporal lobes. Abnormalities were also found in the putamen, lateral thalamus, and pulvinar. Optic tract and radiations were largely spared. These neuropathology findings correspond to those at follow-up MR imaging when our patient was 4 months old, except for the fact that in our patient the occipital lobes were most severely affected. Recently, CT findings have been described in two children with the infantile form of citrullinemia (2). Bilateral and symmetric corticosubcortical hypoattenuating areas, ulegyric changes and atrophy of the frontal lobes, the gyrus cinguli, insulae, and temporal lobes were found. Findings in the occipital lobes, basal ganglia, thalami, and cerebellum were unremarkable. These findings correspond to those at follow-up MR imaging of our patient, except for the fact that in our patient the occipital lobes were most severely affected. Both acute and chronic hyperammonemia have deleterious effects on glutamate receptor function (11). Several studies suggest the existence of a unique ontogenetic profile of susceptibility of the brain to excessive activation of amino acid receptor subtypes (17). The relatively high vulnerability of the occipital lobes in the neonatal form of citrullinemia may relate to the development of receptors for excitatory amino acids that are predominantly located in the occipital lobes in this age group (18).

The differential diagnosis of the MR imaging pattern of damage in the neonatal brain with citrullinemia includes neonatal hypoglycemia and superior sagittal sinus thrombosis (18). MR imaging studies in neonatal hypoglycemia show damage primarily to the parietal and occipital lobes (18) and may resemble those found in citrullinemia. Superior sagittal sinus thrombosis can also cause bilateral paramedian brain injury, but in these cases the thrombus itself can usually be visualized at MR imaging (18). Severe hypoxic-ischemic encephalopathy in neonates has a

different MR imaging pattern, involving predominantly the ventrolateral thalami, the posterior putamina, and the perirolandic regions (19).

Conclusion

Our case illustrates the added value of diffusion-weighted and diffusion tensor imaging in a patient with citrullinemia for the early detection of irreversible brain damage and for the characterization of hyperintense abnormalities on T2-weighted MR images. At the subacute stage, these areas were consistent with cytotoxic edema, as demonstrated at diffusion-weighted imaging. At follow-up MR imaging, they represented damage to the oligodendro-axonal unit, reflected by a decrease in fractional anisotropy in the white matter at diffusion tensor imaging. It is important to realize that severe brain damage in the neonatal period is not always caused by hypoxic-ischemic disease. Metabolic disorders such as urea cycle defects should also be considered.

Acknowledgments

We thank Gerard J. den Heeten, Department of Radiology, Academic Medical Center, Amsterdam, and Peter G. Barth, Department of Pediatric Neurology, Academic Medical Center, Amsterdam, for reviewing the manuscript and providing invaluable comments.

References

1. Wayenberg JL, Vermeylen D, Gerlo E, Pardou A. **Increased intracranial pressure in a neonate with citrullinaemia.** *Eur J Pediatr* 1992;151:132–133
2. Albayram S, Murphy KJ, Gaillod P, et al. **CT Findings in the infantile form of citrullinemia.** *AJNR Am J Neuroradiol* 2002;23:334–336
3. Osafune K, Ichikawa K, Yasui T, et al. **An adult-onset case of argininosuccinate synthetase deficiency presenting with atypical citrullinemia.** *Intern Med* 1999;38:590–596
4. Kawata A, Suda M, Tanabe H. **Adult-onset type II citrullinemia: clinical pictures before and after liver transplantation.** *Intern Med* 1997;36:408–412
5. Chen YF, Huang YC, Liu HM, Hwu WL. **MRI in a case of adult-onset citrullinemia.** *Neuroradiology* 2001;43:845–847
6. Oshiro S, Kochinda T, Tana T, et al. **A patient with adult-onset type II citrullinemia on long-term hemodialysis: reversal of clinical symptoms and brain MRI findings.** *Am J Kidney Dis* 2002;39:189–192
7. Akkerman EM. **Efficient measurement and calculation of MR diffusion anisotropy images using the platonic variance method.** *Magn Reson Med* 2003;49:599–604
8. Saheki T, Kobayashi K, Inoue I. **Hereditary disorders of the urea cycle in man: biochemical and molecular approaches.** *Rev Physiol Biochem Pharmacol* 1987;108:21–68
9. Martin JJ, Farriaux JP, De Jonghe P. **Neuropathology of citrullinemia.** *Acta Neuropathol (Berl)* 1982;56:303–306
10. Voorhies TM, Ehrlich ME, Duffy TE, et al. **Acute hyperammonemia in the young primate: physiologic and neuropathologic correlates**. *Pediatr Res* 1983;17:970–975
11. Felipo V, Butterworth RF. **Neurobiology of ammonia.** *Prog Neurobiol* 2002;67:259–279
12. Gutierrez JA, Truemper EJ, Burton EM, Mercado-Daene MG. **Perinatal pathology casebook.** *J Perinatol* 1996;16:77–79
13. Okken A, Van der Blij JF. **Citrullinemia and brain damage.** *Pediatr Res* 1973;7:52–53
14. Pierpaoli C, Jezzard P, Basser PJ, et al. **Diffusion tensor MR imaging of the human brain.** *Radiology* 1996;20:637–648
15. Schaefer PW, Grant PE, Gonzalez RG. **Diffusion-weighted MR imaging of the brain.** *Radiology* 2000;217:331–345
16. Huppi PS, Murphy B, Maier SE, et al. **Microstructural brain development after perinatal cerebral white matter injury assessed by diffusion tensor magnetic resonance imaging.** *Pediatrics* 2001;107:455–460
17. Naidu SB, Moser HW. **Value of neuroimaging in metabolic diseases affecting the CNS.** *AJNR Am J Neuroradiol* 1991;12:413–416
18. Barkovich AJ, Ali FAA, Rowley HW, Ross N. **Imaging patterns of neonatal hypoglycemia.** *AJNR Am J Neuroradiol* 1998;19:523–528
19. Barkovich AJ, Westmark K, Patridge C, et al. **Perinatal asphyxia: MR findings in the first 10 days.** *AJNR Am J Neuroradiol* 1995;16:427–438